Soliton-plasmon resonances as Maxwell nonlinear bound states

C. Milián,[1,2,*] D. E. Ceballos-Herrera,[3] D. V. Skryabin,[2] and A. Ferrando[4]

[1]*Instituto de Instrumentación para Imagen Molecular (I3M), InterTech, Universitat Politècnica de València, Camino de Vera S/N, Valencia 46022, Spain*

[2]*Centre for Photonics and Photonic Materials, Department of Physics, University of Bath, Bath BA2 7AY, UK*

[3]*Universidad Autónoma de Nuevo León, Facultad de Ciencias Físico Matemáticas, Avenida Universidad S/N, Cd. Universitaria, Nuevo León 66450, México*

[4]*Departament d'Òptica, Interdisciplinary Modeling Group InterTech, Universitat de València, Dr. Moliner 50, Burjassot, València 46100, Spain*

**Corresponding author: cme22@bath.ac.uk*

Received July 25, 2012; revised September 3, 2012; accepted September 4, 2012; posted September 5, 2012 (Doc. ID 173035); published October 5, 2012

We demonstrate that soliplasmons (soliton–plasmon bound states) appear naturally as eigenmodes of nonlinear Maxwell's equations for a metal/Kerr interface. Conservative stability analysis is performed by means of finite element numerical modeling of the time-independent nonlinear Maxwell equations. Dynamical features are in agreement with the presented nonlinear oscillator model. © 2012 Optical Society of America

OCIS codes: 190.6135, 240.6680.

Nanoscaled plasmonic optical solitons have attracted much attention in the last few years. Recent studies report plasmonic solitons in single and double metal/dielectric interfaces [1,2], systems with gain and loss [3,4], waveguide arrays [5–7], and chains of nanoparticles [8]. Strong surface plasmon polariton (SPP) fields at the interface enhance the nonlinear effect [9].

Recently, it has been suggested that SPPs can couple to spatial solitons [10] because both have a wavenumber greater than that of the light cone (see, e.g., [11–13]) and their dispersion relations intersect [see Fig. 1(b)]. A symmetric coupled oscillator model was introduced by means of heuristic reasoning, and its dynamical properties were fully analyzed in [14]. Although surface solitons were earlier studied (see, e.g., [15,16]), they consisted of one component only, whereas the soliplasmons considered here consist of two: one peaked at the metal interface and the other one peaked far from it in the Kerr medium.

In this Letter, we prove for the first time that the soliplasmons proposed in [10] exist in the context of Maxwell equations. We compute numerically the soliplasmons as eigenstates of the nonlinear Maxwell equations for a metal/Kerr interface [Fig. 1(a)], showing that they are classified according to the relative soliton–plasmon phase $\delta = 0, \pi$. Finite element analysis modeling is used to integrate the time-independent nonlinear Maxwell equations in two dimensions to analyze soliplasmon stability. The non-self-adjoint character of the Maxwell operator (property of the vectorial nature of the system) leads to an oscillator model with asymmetric coupling between the SPP and the soliton. This model has no unknown parameters (as opposed to [10]) and therefore predicts realistic physical properties of the stationary solutions and their stability. Inclusion of ohmic losses is observed to yield a nontrivial dynamics.

We analyze the full-vector nonlinear equation for a monochromatic wave (cw) $\mathbf{E}_\omega$ with frequency $\omega = ck$,

$$\left[\frac{\partial^2}{\partial z^2} + \frac{\partial^2}{\partial x^2} + k^2\varepsilon_L(x)\right]\mathbf{E}_\omega = \mathcal{L}_v(x)\mathbf{E}_\omega - \mathbf{P}_{\mathrm{NL}}, \quad (1)$$

where $\varepsilon_L = \varepsilon_{m(K)}$ for $x < 0$ ($x > 0$), $\mathcal{L}_v \equiv \nabla[\nabla\circ]$, $\mathbf{P}_{\mathrm{NL}} = [k^2\chi^{(3)}/3]\{2|\mathbf{E}_\omega|^2\mathbf{E}_\omega + \mathbf{E}_\omega^2\mathbf{E}_\omega^*\}$, and $\chi^{(3)} \equiv \varepsilon_0 c\varepsilon_K n_2$. Our geometry is assumed to be illuminated from the Kerr medium [see Fig. 1(a)], and diffraction along y is neglected. Equation (1) can be transformed into the dynamical equations of a soliplasmon by using the variational *ansatz* of [10],

$$\mathbf{E}_\omega(x,z) = [c_p(z)\mathbf{e}_p(x) + \mathbf{u}c_s(z)f_s(x-a;c_s(z))]e^{ikn_K z}, \quad (2)$$

where c_p, c_s are the complex amplitudes. $\mathbf{e}_p(x)$ is a TM-SPP on the interface with propagation constant β_p, which is a stationary solution of Eq. (1), and hence $c_p(z) = c_p(0)e^{i\mu_p z}$ ($\beta_p = kn_K + \mu_p$). The soliton term in Eq. (2), $\phi_s = c_s f_s = c_s\,\mathrm{sech}(\kappa_s[x-a])$, $\kappa_s \equiv [kn_K\gamma]^{1/2}|c_s|$, is located at a distance a from the interface, such that the overlap with the SPP is small (weak coupling), and it is a solution of the stationary scalar ($\mathcal{L}_v = 0$) and paraxial nonlinear Schrödinger equation, $\{1/[2kn_K]\partial_x^2 + \gamma|\phi_s|^2\}\phi_s = \mu_s\phi_s$ ($\gamma \equiv k\chi^{(3)}/[2n_K]$), with $c_s(z) = c_s(0)e^{i\mu_s z}$

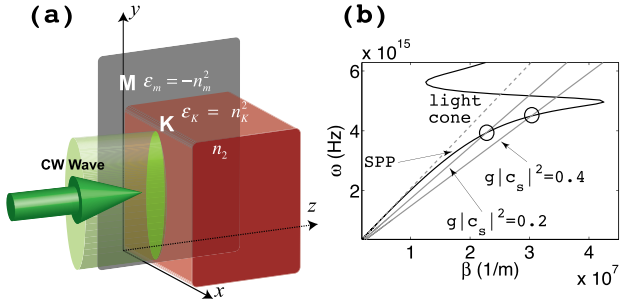

Fig. 1. (Color online) (a) Metal/Kerr structure with linear dielectric constants $\varepsilon_m = -n_m^2$, $\varepsilon_K = n_K^2$ and nonlinear Kerr index n_2. (b) Dispersion of a SPP in a lossy metal (black) and a spatial soliton (gray) owning two different amplitudes ($\beta_s = kn_K[1 + g|c_s|^2]$). Circles enclose the matching points, and the dashed line marks the light cone $\omega = \beta c/\sqrt{\varepsilon_K}$.

and $\beta_s = kn_K + \mu_s$, where $\mu_s = \gamma|c_s(0)|^2/2$. Note that $c_s(z)$ appears nonlinearly in Eq. (2), which prevents the soliplasmon from behaving as a linear superposition of the two modes. Considering that a is constant and that the soliton is x-polarized, i.e., $\mathbf{u} \approx \mathbf{x}$, (as supported by Figs. 3–5), substitution of Eq. (2) in the paraxial version of Eq. (1), $-i\partial_z e_x = \hat{M} e_x$, leads to the soliplasmon equations [17] ($\dot{\Psi} \equiv d\Psi/dz$)

$$-i|\dot{c}\rangle = M|c\rangle, \qquad M = [\hat{M}] = \begin{bmatrix} \mu_p & q(|c_s|) \\ \bar{q}(|c_s|) & \mu_s \end{bmatrix}, \quad (3)$$

where $|c\rangle \equiv [c_p, c_s]^T$. The origin of the coupling in Eq. (3) is the nonorthogonality relation $\int_x e_{px}^* f_s \neq 0$, and it is not symmetric in general, $\bar{q}/q \sim N_p/N_s$, where $q \equiv k/[2n_K N_p] \int_x [\varepsilon_L - n_K^2]\mathbf{e}_p \mathbf{u} f_s \sim \exp(-a\sqrt{kn_K\gamma}|c_s|)$, $N_p \equiv \int_x |e_{px}|^2$ and $N_s \equiv \int_x f_s^2$. This feature was not captured by previous heuristic models [10,14]. Interestingly, q, $\bar{q}$ are proportional to the value of the soliton tail at the interface [10], revealing that a *strong* soliton drives a *weak* SPP ($N_s \gg N_p$) at a rate q.

Stationary soliplasmons of Eq. (3) are determined from the eigenvalues, μ_δ, and eigenvectors, $|\mu_\delta\rangle = c_{s0}[q/\{\mu_\delta - \mu_p\}, 1]^T$ of M ($c_{s0} \in \mathrm{C}$),

$$\beta = kn_K + \bar{\mu} + e^{i\delta}\sqrt{\Delta_\mu^2 + q\bar{q}}, \qquad \delta = 0, \pi, \quad (4)$$

$$\frac{E_x(x,z)}{c_{s0}} = \left\{\frac{q e_{px}(x)}{\mu_\delta - \mu_p} + \mathrm{sech}(\kappa_s[x-a])\right\} e^{i\beta z}, \quad (5)$$

where $\beta = kn_K + \mu_\delta$, $\bar{\mu} \equiv [\mu_p + \mu_s]/2$, and $\Delta_\mu \equiv [\mu_p - \mu_s]/2$. Note from Eq. (4) that $\mu_0 > \mu_p$ and $\mu_\pi < \mu_p$, so the plasmon term in Eq. (5) is >0 (<0) for $\delta = 0$ (π) and δ is the relative soliton–plasmon phase. The minimum value of $\mu_\delta - \mu_p = \sqrt{q\bar{q}}\exp(i\delta)$ imposes a maximum in the soliplasmon norm, the solution with infinite power $\mu_\delta = \mu_p$ being nonphysical. We verified these features by plotting the guided power $P(\mu;\omega,a) = \int_x E_x^* H_y/2 = \omega\varepsilon_0/[2\beta]\int_x \varepsilon|E_x|^2$ of the numerically computed soliplasmons in Fig. 2. At fixed (ω, a) there are two divergent branches, $\mu_0 > \mu_p$ (right) and $\mu_\pi < \mu_p$ (left), in agreement with Eq. (4). Far from the asymptote, both branches coalesce into the monotonically increasing soliton curve $P_s(\mu) \sim \mu^{1/2}$, but close to it they open a gap in μ, which is proportional to $\sqrt{q\bar{q}} \sim \exp(-a\sqrt{kn_K\gamma}|c_s|)$. Soliplasmons are computed from Eq. (1) ($\mathbf{E}(x,z) = \mathbf{E}(x)e^{i\beta z}$) on a silver/glass interface ($\epsilon_m = -82$, $\epsilon_K = 2.09$, $n_2 = 2.6\times10^{-20}$ m^2/W), by means of an iterative Fourier method that fixes a, letting the families $P(\mu;a)$ be found separately. Soliplasmons with $\delta = 0, \pi$ naturally appear (see insets of Fig. 2).

The stability of soliplasmons was checked by propagating the solutions with input noise (20% in amplitude) and without losses ($\epsilon_m \in \mathrm{Re}$). Focusing a beam into the Kerr material is likely to excite soliplasmons with a strong solitonic component, so we focus below on the case $N_p/N_s \ll 1$ ($\bar{q} \ll q$), in which the soliton dynamics is quasi-stationary; i.e., $|\dot{c}_s|/|c_s| \ll |\dot{c}_p|/|c_p|$. In this situation, the dynamics can be qualitatively predicted by

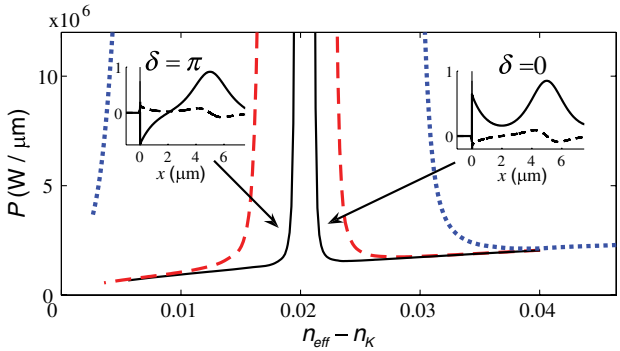

Fig. 2. (Color online) P versus μ/k curves for $\delta = 0$ (right) and $\delta = \pi$ (left) soliplasmon families at $\omega \simeq 1.26$ PHz ($\lambda = 1.5$ μm) for $a = 3$ μm (dotted), $a = 4$ μm (dashed), and $a = 5$ μm (solid). Insets: x (solid) and z (dashed) dimensionless components of the mode profiles $\mathcal{E} \equiv \sqrt{\chi^{(3)}}\mathbf{E}_\omega$.

rewriting Eq. (3) as two equations for the relative phase, $\phi_{sp} \equiv \phi_p - \phi_s$, and $|c_p|$ ($c_{p,s} = |c_{p,s}|\exp(i\phi_{p,s})$),

$$\dot{\phi}_{sp} \approx 2\Delta_\mu + q\frac{|c_s|}{|c_p|}\cos\phi_{sp}, \qquad |\dot{c}_p| = q|c_s|\sin\phi_{sp}. \quad (6)$$

Perturbations introduced here induce an increase of ϕ_{sp} [see Figs. 4(b) and 5(b)]. The amplitude Eq. (6) predicts that in this situation $|c_p|$ will increase (decrease) if $\sin\phi_{sp} > 0$ (<0). These features are clear in our dynamical simulations, which integrate Eq. (1) with no approximations and permit us to evaluate c_p, c_s as the peak amplitudes of the plasmon and soliton components. Figure 3 shows the propagation of a $\delta = \pi$ solution. Apart from being diffraction free, the input noise introduces fluctuations that propagate away from the soliplasmon

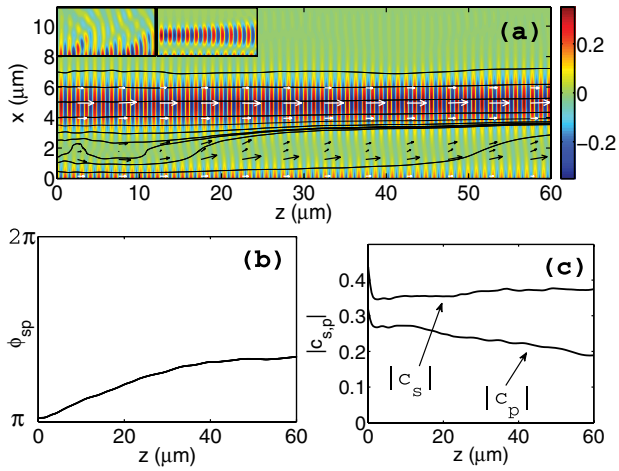

Fig. 3. (Color online) (a) $\mathcal{E}_x$ of the π-soliplasmon with $n_{\mathrm{eff}} = 1.464$ along propagation. Left inset magnifies $\mathcal{E}_x$ over the area where it is placed. Contour lines of the Poynting vector norm show power flow, the magnitude of which is represented by the arrows, with the black ones being magnified. Right inset shows the diffraction observed in the linear regime over the first 12 μm. (b) Phase, ϕ_{sp}, and (c) amplitudes, $|c_{s,p}|$, associated to (a). Initial jumps in (c) are due to input noise.

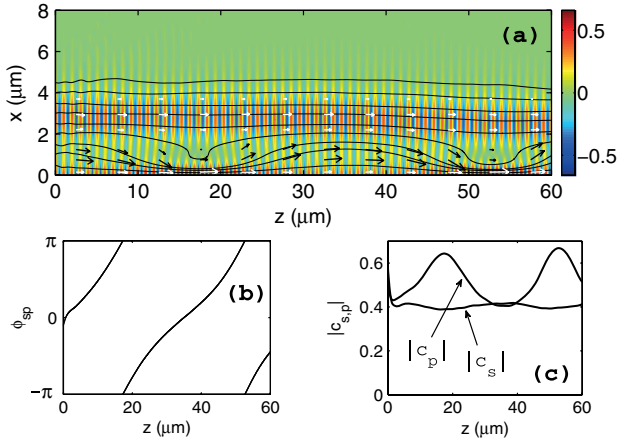

Fig. 4. (Color online) Propagation of the 0-soliplasmon with $n_{\text{eff}} = 1.472$. (a) $\mathcal{E}_x$, (b) soliton–plasmon relative phase, and (c) soliton and plasmon amplitudes.

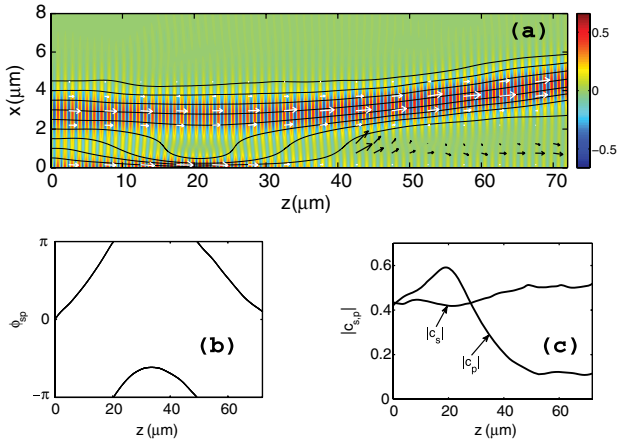

Fig. 5. (Color online) Propagation under the initial conditions of Fig. 4, including ohmic losses, $\text{Im}\{\epsilon_m\} = 8.3$.

(see insets). The decrease of $|c_p|$ is associated to the transfer of energy from the SPP to the soliton.

Propagation of a $\delta = 0$ solution (see Fig. 4) shows a very different behavior, since the initial increase of $|c_p|$ implies that the SPP drains energy from the soliton. Remarkably, $|\dot{c}_p| = 0$ at $\phi_{sp} = 0, \pm\pi$ and the flow of energy between the soliton and SPP is reversed [see Figs. 4(b), 4(c)], as Eq. (6) predicts. $\delta = \pi$ soliplasmons appear to be more oscillatory stable than the $\delta = 0$ ones, stability meaning a small energy transfer between the soliton and SPP components.

The effect of ohmic losses is shown in Fig. 5, for the same initial conditions of Fig. 4. The first ~20 μm present similar dynamics in both cases. However, as soon as $\phi_{sp} = \pi$, the soliton stops pumping the SPP and $|c_p|$ drops dramatically [compare with Fig. 4(c)]. Exposure to metal reflection bends the soliton trajectory and decouples it from the SPP. Therefore, losses may induce a significant drift of the soliton position, a, and a realistic dynamical model has to consider it as a variational parameter too. This issue is subject of current work.

In summary, we reported on the progress made towards the analysis of the stationary and dynamical properties of soliton–plasmon bound states, *soliplasmons*, by means of numerical modeling of Maxwell equations. The oscillator model introduced predicts qualitatively the physics associated to these waves.

The work of A. F. and C. M. was partially supported by the Ministerio de Ciencia e Innovación (MICINN) TEC2010-15327 project.

References and Notes

1. A. R. Davoyan, I. V. Shadrivov, and Y. S. Kivshar, Opt. Express **17**, 21732 (2009).
2. E. Feigenbaum and M. Orenstein, Opt. Lett. **32**, 674 (2007).
3. A. Marini, D. V. Skryabin, and B. Malomed, Opt. Express **19**, 6616 (2011).
4. A. Marini and D. V. Skryabin, Phys. Rev. A **81**, 033850 (2010).
5. F. Ye, D. Mihalache, B. Hu, and N. C. Panoiu, Phys. Rev. Lett. **104**, 106802 (2010).
6. J. R. Salgueiro and Y. S. Kivshar, Appl. Phys. Lett. **97**, 081106 (2010).
7. C. Milián and D. V. Skryabin, Appl. Phys. Lett. **98**, 111104 (2011).
8. R. E. Noskov, P. A. Belov, and Y. S. Kivshar, Phys. Rev. Lett. **108**, 093901 (2012).
9. D. V. Skryabin, A. V. Gorbach, and A. Marini, J. Opt. Soc. Am. B **28**, 109 (2011).
10. K. Y. Bliokh, Y. P. Bliokh, and A. Ferrando, Phys. Rev. A **79**, 041803 (2009).
11. A. V. Zayats, I. I. Smolyaninov, and A. A. Maradudin, Phys. Rep. **408**, 131 (2005).
12. S. A. Maier, *Plasmonics: Fundamentals and Applications* (Springer, 2007).
13. Y. S. Kivshar and G. P. Agrawal, *Optical Solitons. From Fibers to Photonic Crystals* (Academic, 2003).
14. Y. Ekşioğlu, O. E. Müstecaplioğlu, and K. Güven, Phys. Rev. A **84**, 033805 (2011).
15. V. M. Agranovich, V. S. Babichenko, and V. Ya. Chernyak, Sov. Phys. JETP Lett. **32**, 512 (1981).
16. W. J. Tomlinson, Opt. Lett. **5**, 323 (1980).
17. Details on this derivation will be reported elsewhere.